

Dynamics of Magnetic Bead Chain in Magnetic Field

Hiroyuki Kawamoto, Nobuyuki Nakayama and Makoto Yamaguchi
Department of Mechanical Engineering, Waseda University
Shinjuku, Tokyo, Japan

Abstract

Experimental, theoretical, and numerical investigations have been carried out on dynamics of a magnetic bead chain in the magnetic field. Chains formed on a solenoid coil were vibrated by the sine-wave excitation method and the resonance frequency was measured. It showed little dependency on the magnetic flux density and the bead diameter, because both the equivalent stiffness and the length of the chain came to large in accordance with the increase of the magnetic flux density. These characteristics were quantitatively confirmed by the theoretical consideration based on the assumption of potential energy minimization and the numerical calculation with the Distinct Element Method. The investigation is expected to be utilized for the improvement of the two-component magnetic brush development subsystem in electrophotography.

Introduction

A magnetic brush development system^{1,2} is most widely used for high-speed color laser printers. A typical schematic of this system is shown in Figure 1. Magnetic carrier beads with electrostatically attached toner particles are introduced into the vicinity of a rotatory sleeve with a stationary magnetic roller inside it. Carrier beads form chains on a sleeve by virtue of the magnetic field. Tips of chains touch the photoreceptor surface at the development area and toner particles on chains move to electrostatic latent images on a photoreceptor to form real images. Carrier chains play an important role in this development step. In order to realize high quality imaging, it is necessary to clarify the relationship between kinetic characteristics of formed chains and design parameters, such as magnetic flux density and properties of carriers. In this study, following the static investigation,³ experimental, numerical, and theoretical investigations have been carried out on dynamics of the chain.

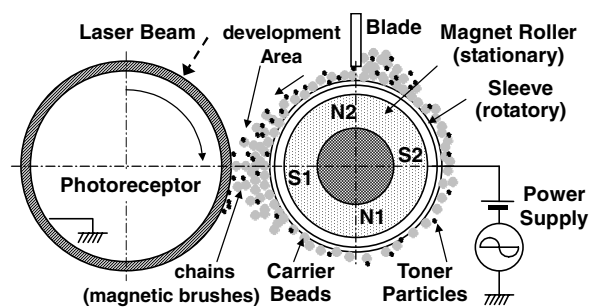


Figure 1. Magnetic brush development system in a laser printer.

Experimental

Experimental Procedure

An experimental set-up and its photograph are shown in Figure 2 and Figure 3, respectively. A solenoid coil with carrier chains was mounted on a shaker (Shinken Co., G14-818), and vibration of chains was observed through a microscope camera (Keyence Corp., VH-7000). Five kinds of spherical carriers were used for experiments. These are made by the polymerization method with 18, 35, 55, 88, and 107 μm in diameter, 3500-3620 kg/m^3 volume density, and 4.2-4.7 in relative magnetic permeability (Toda Kogyo Corp.). Photograph of one of them (107 μm in diameter) is shown in Figure 4(a). Carrier beads were initially arranged at the center of a plastic plate on the coil end in a $\phi 10$ mm area. Axial magnetic flux density B' along the center axis of the coil was measured by a separate experiment and approximated by $B'(z) = B_0(1-cz)$, where B_0 and c ($= 66.87$ 1/m) are constants and z (m) is the axial coordinate ($z = 0$ at the surface of the end plate on which carrier beads were mounted). B_0 is proportional to the coil current with a proportional constant 0.006156 T/A. The coil was excited in two directions: one is axial excitation and another is radial as shown in Figure 2. The shaker was operated with sine wave and the frequency was swept up and down from 10 to 90 Hz.

Resonant frequency of bulk chains was not single but it distributed in wide range, because characteristics of chains were not identical but bulk chains contained long and short, as shown in Figure 4(b), and softly and hardly connected chains. This feature made the determination of the resonant frequency very difficult. In this experiment, averaged data observed by four persons at three times were adopted as representatives. It should be emphasized that data contained very large error.

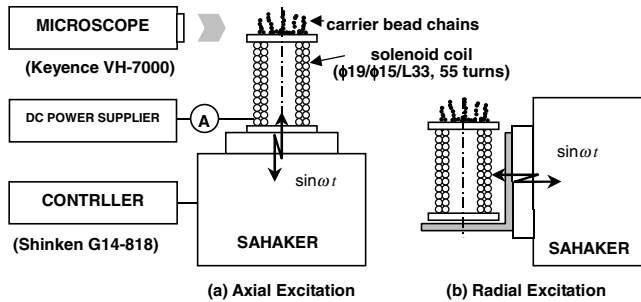


Figure 2. Experimental set-up to measure resonance frequency of bead chains in magnetic field.

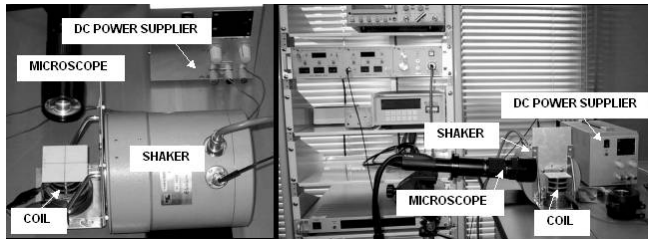


Figure 3. Photographs of experimental set-up.

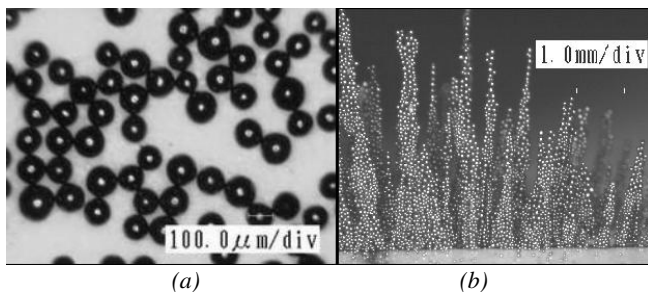
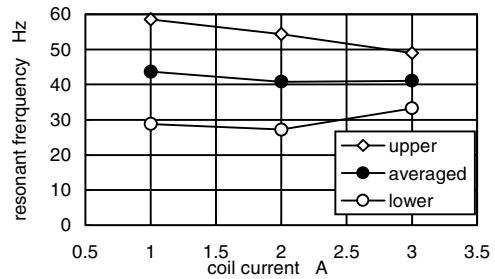


Figure 4. (a) Magnetic carrier beads (107 μm diameter) and (b) chains in magnetic field (88 μm diameter, in 3 A field).

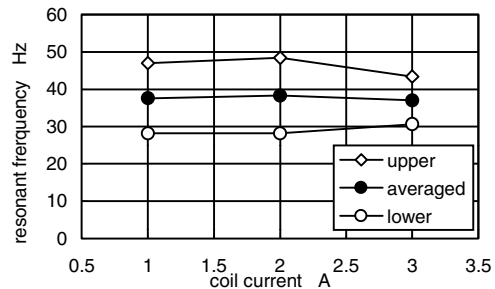
Experimental Results

Axial Excitation. Axial excitation experiments were conducted under conditions of 1.5 Hz/s sweep up and down rate and constant magnitude (0.4 mm) of vibration. Although excitation acceleration exceeded 1 G over 25 Hz, chains did not break nor jump, because magnetic attractive

force was larger than axial excitation force. Radial resonant vibration was observed even though chains were excited in the axial direction, because the excitation was not exactly axial but it contained a radial component and chains were not perpendicular to the axial direction except at the center. Figure 5 shows observed resonance frequency. Lower and upper limits of the vibration occurrence were cited 'lower' and 'upper,' respectively. Although the resonant frequency laid in wide range and small hysteresis existed, it roughly suggested that the resonant frequency did not depend on the intensity of the magnetic field. Figure 6 shows a relationship between particle size and the averaged resonant frequency. Particle size also did not influence the resonance frequency.



(a) measured during speed-up period



(b) measured during speed-down period

Figure 5. Resonant frequency measured by axial excitation method. (88 μm diameter, 0.05 g @ φ 10 mm)

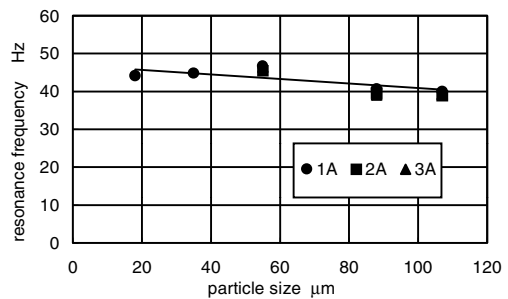


Figure 6. Relationship between particle size and resonance frequency. (0.05 g @ φ 10 mm)

Equivalent stiffness of the chain was evaluated from experimental data. The chain was assumed to be a cone shape and an equivalent mass of the chain m_c was estimated from the measured chain length and bottom width. These are shown in Figure 7. Bulk density of the chain was assumed to be 0.5. The equivalent stiffness was calculated from $m_c(2\pi f)^2$ and shown in Figure 8, where f is the measured resonance frequency shown in Figure 5. It is recognized from Figure 8 that the stiffness of the chain was high in high magnetic field. This is because the magnetic force between beads becomes high in high magnetic field. Because both the mass and the stiffness of the chain increased with the magnetic field strength, the resonance frequency was almost independent on the magnetic field strength.

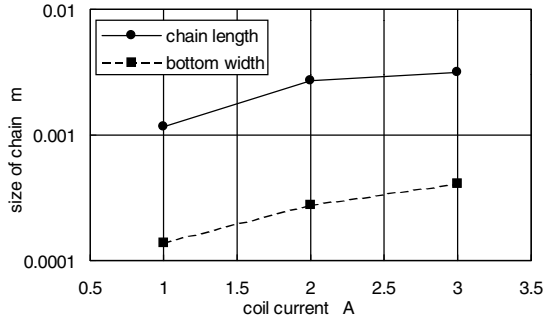


Figure 7. Characteristic sizes of chain. (88 μm diameter, 0.05 g @ ϕ 10 mm)

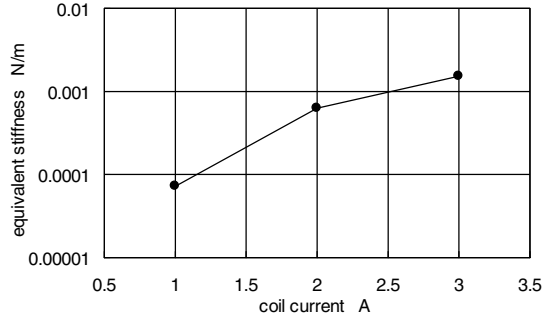
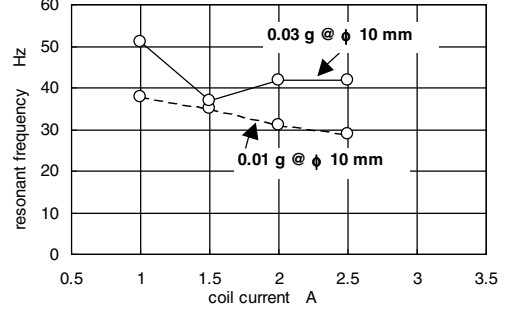


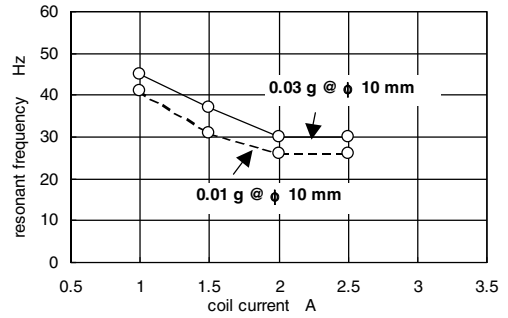
Figure 8. Equivalent stiffness of chain. (88 μm diameter, 0.05 g @ ϕ 10 mm)

Radial Excitation. Radial excitation experiments were conducted under almost the same conditions except that constant acceleration (1-3 m/s^2) scheme was employed in this experiment. Measured frequencies of the lower limit are shown in Figure 9. Because the chain shifted laterally at high excitation frequency, the upper limit of the resonant frequency could not be observed. Repulsive force between the adjacent chains⁴ is the cause of the lateral movement. In any case, the resonant frequency was almost independent on

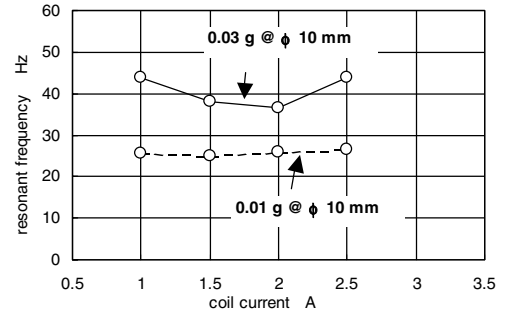
the magnetic field strength and bead diameter. These characteristics agreed qualitatively with those of the axial excitation experiment.



(a) 35 μm bead diameter



(b) 88 μm bead diameter



(c) 107 μm bead diameter

Figure 9. Resonant frequency measured by radial excitation method.

Theoretical

It is assumed that chain lengths are determined to minimize its total potential energy given by the sum of magnetic energy U_m and gravitational energy U_k .

$$U_m = -\frac{1}{2} \sum_{j=1}^N m_j \cdot B_j', \quad U_k = g \sum_{j=2}^N m_{b,j} \left(\sum_{k=1}^{N-1} a_k + \frac{a_N}{2} \right), \quad (1)$$

where N is a total number of beads, g is the gravitational constant, m_{bj} is the mass of j -th bead, and a_j is the diameter of the j -th bead. The magnetic moment m_j at the position of the j -th particle is

$$m_j = \frac{4\pi}{\mu_0} \frac{\mu - 1}{\mu + 2} \frac{a^3}{8} B_j + \frac{\mu - 1}{\mu + 2} \frac{a^3}{8} \sum_{\substack{k=1 \\ k \neq j}}^N \left[3 \frac{(m_k \cdot r_{kj})}{r_{kj}^5} r_{kj} - \frac{m_k}{r_{kj}^3} \right] \quad (2)$$

where μ_0 is the permeability of free space and μ is the relative permeability of beads. The first term in the right hand side of Equation (2) is due to the applied magnetic field by the coil and the second term is generated at the j -th bead by the field due to dipoles of other beads. Although the assumption is not exactly right because the system is not a potential field but irreversible, it roughly approximates the static chain formation in the magnetic field.³ Based on this concept it is also assumed, as a first order approximation, that the equivalent stiffness of the chain is proportional to the total potential energy per a bead. Figure 10 shows calculated relative resonance frequency, where beads are assumed to be connected along a straight line in vertical. Although the resonant frequency was not constant with respect to the magnetic field strength and the bead diameter, the dependencies were small.

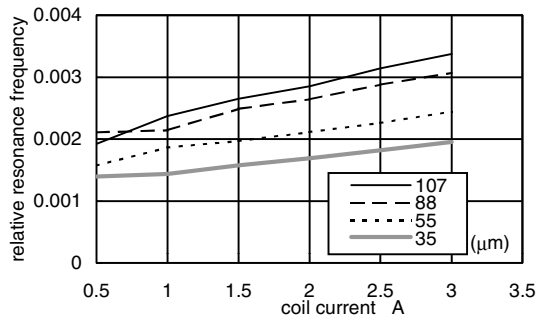


Figure 10. Resonance frequency of chain in magnetic field based on the concept of potential energy minimization. The ordinate is relative.

Numerical Simulation

Numerical Method

Two-dimensional Distinct Element Method (DEM) was used in the numerical simulation of dynamic behavior of the magnetically formed chain. In the calculation the momentum equations are solved with three degrees of freedom for each bead. In this study, mechanical interaction force, magnetic force, drag due to air flow, and gravity are considered in the equations but the effect of rolling friction and van der Waals force are neglected. Mechanical

interaction force is calculated by the Hertz's formula. The magnetic force F_j and rotational moment M_j of the j -th bead with the magnetic moment m_j are given by the following expressions under the assumption that each bead behaves as a magnetic dipole placed at the center of the magnetized bead.

$$F_j = (m_j \cdot \nabla) B_j, \quad M_j = m_j \times B_j. \quad (3)$$

The magnetic flux density B_j at the position of the j -th bead is

$$B_j = B_j + \sum_{\substack{k=1 \\ k \neq j}}^N \frac{\mu_0}{4\pi} \left[3 \frac{(m_k \cdot r_{kj})}{r_{kj}^5} r_{kj} - \frac{m_k}{r_{kj}^3} \right]. \quad (4)$$

Although the actual chain was a cone or tower shape, a single row of beads was assumed in the calculation to evaluate the effect of the magnetic flux density and the chain length separately. Calculation conditions are; Young's modulus of beads = 10 GPa, Young's modulus of plate = 100 GPa, Poisson's ratio = 0.3, and friction coefficient = 0.2. Diameter, density, and magnetic permeability of beads were adjusted with the measured.

Numerical Results

A step force was applied to the chain and the response of the chain deformation was calculated. The bottom bead was fixed to the plate to prevent lateral shift of the total chain and the magnitude of acceleration was adjusted not to break down the chain. One example of calculation is shown in Figures 11 and 12. Figure 11 is time-step variation of chain profile and Figure 12 is the vibration response of the top bead. Because the bead row was assumed to be single, a slope was highest at the lowest bead and the mode of vibration was not the same with that of the actual chain. The resonance frequency was 20.8 Hz in this case.

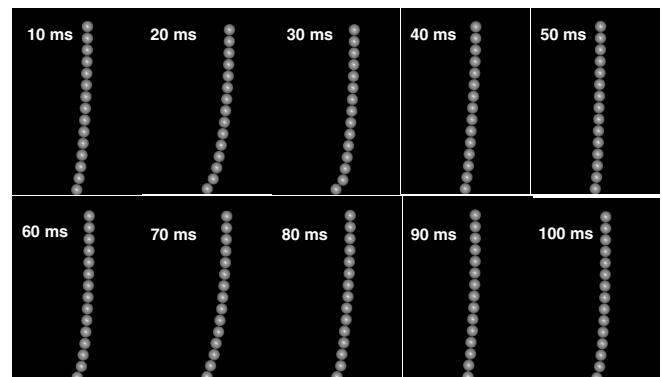


Figure 11. Time variation of chain profile. (15 beads, 3 A, 1.7 m/s² acceleration)

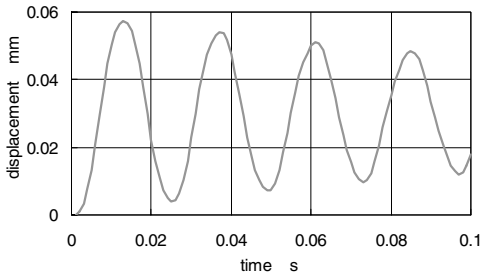


Figure 12. Horizontal displacement of top bead. Calculation conditions are common with those of Figure 11.

Parametric calculation was conducted to examine effects of the magnetic field strength and the bead length. Figure 13 shows vibration responses of 5-bead chain in 1, 2, and 3 A coil-current fields and Figure 14 is the deduced stiffness of the chain. It is evident that the frequency and therefore the stiffness became higher in the higher magnetic field, if the number of beads was constant even when the magnetic field became high.

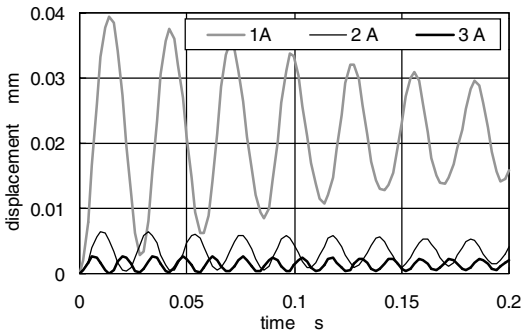


Figure 13. Horizontal displacements of 5-bead chain in different magnetic field.

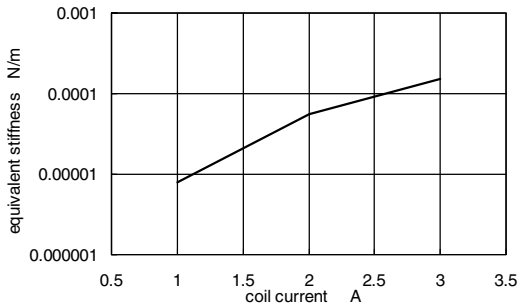


Figure 14. Stiffness of 5-bead chain.

The next calculation is to examine effect of bead length. Figure 15 is vibration responses of chains that consist of 3, 5, and 7 beads in the common field (1 A coil current) and Figure 16 is the deduced stiffness of the chain.

The frequency and therefore the stiffness was low when the chain was long.

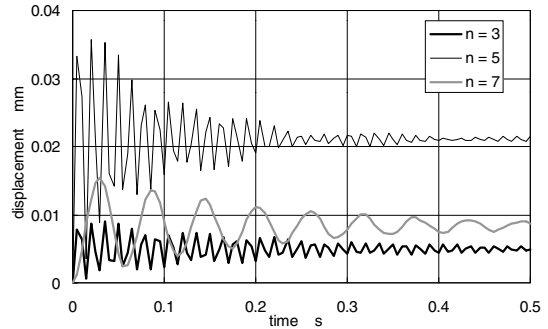


Figure 15. Horizontal displacements of chains that consist of different number of beads in the common magnetic field. (1 A)

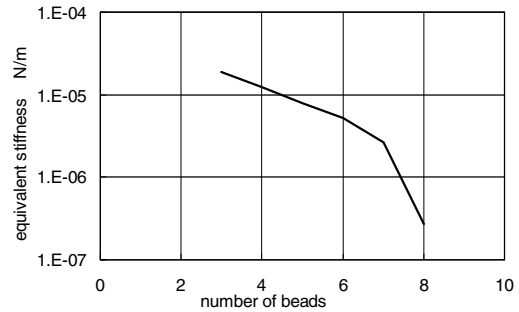


Figure 16. Stiffness of chain in common field. (1 A)

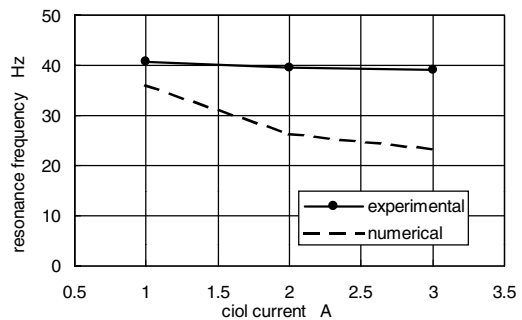


Figure 17. Calculated and measured resonance frequency. (88 μm diameter)

Combining two calculation results on the effect of the magnetic field and the chain length, we can deduce the resonance frequency of the chain that consists of the realistic number of beads based on the experimental result in Figure 7. Figure 17 shows the comparison of the calculated and measured resonance frequency. Numerical calculation was conducted with the half-length chain corresponding to those of Figure 7 to avoid dynamic break

down of chain. This occurred because the single row of beads was assumed whereas the actual chain was the stable cone shape. In any case, The calculated resonance frequency was almost independent on the field strength that qualitatively agreed with the measured and theoretical results.

Concluding Remarks

Experimental, theoretical, and numerical studies have been carried out on dynamics of a magnetic bead chain in the magnetic field to utilize for the improvement of the two-component magnetic blush development subsystem in electrophotography. Although the present investigation was preliminary, it has been deduced that both the equivalent stiffness and the length of the chain came to large in accordance with the increase of the magnetic flux density and therefore the resonance frequency of the chain showed little dependency on the magnetic flux density and the bead diameter. Further investigation is being conducted on the measurement of vibration response of the chain by a laser displacement meter and the DEM calculation for realistic cone-shape chains.

Acknowledgement

The authors would like to express their thanks to the Ministry of Education, Science and Culture of Japan for the financial support, to Toda Kogyo Corp. for supplying carrier beads, and to Janjomsuke Wiphut (Bank of Thailand), N. Sukou, S. Yamada, and A. Sasakawa (Waseda Univ.) for their help of carrying out experiments.

References

1. E. M. Williams, *The Physics and Technology of Xerographic Processes*, Krieger Publishing, FL (1993).
2. L. B. Schein, *Electrophotography and Development Physics* (Revised Second Edition), Laplacian Press, CA (1996).
3. N. Nakayama, H. Kawamoto and M. Yamaguchi, Statics of Magnetic Bead Chain in Magnetic Field, *NIP17* (2001).
4. R. S. Paranjpe and H. G. Elrod, Stability of chains of permeable spherical beads in an applied magnetic field, *J. Appl. Phys.*, **60** (1986), 418-422.

Biography

KAWAMOTO, Hiroyuki holds a BS degree in Electrical Engineering from Hiroshima Univ. (1972) and a Dr. degree in Mechanical Engineering from Tokyo Institute of Technology (1983). From 1972 to 1991 he was a Senior Engineer at the Nuclear Division of Hitachi Ltd. In 1991 he moved to Fuji Xerox, and had been engaged in the research of electrophotography as a Research Fellow. In 1999 he left Fuji Xerox and he is now a professor of Waseda Univ. His awards include the Japan Society of Mechanical Engineers Young Scientist Award (1984), the 7th International Microelectronics Conf. Best Paper Award (1992), the Japan Institute of Invention and Innovation Patent Award (1993), and the 10th International Symposium on Applied Electromagnetics and Mechanics Award for Outstanding Presentation Paper (2001). He was selected a Fellow of the IS&T in 1999.